DesignCon 2017

Back to basics: the onset of skin effect in circuit board traces

Eric Bogatin, Teledyne LeCroy Signal Integrity Academy
eric@beTheSignal.com

Yuriy Shlepnev, Simberian Inc.
shlepnev@simberian.com

Chun-Ting "Tim" Wang Lee
chunting.wanglee@colorado.edu
timwanglee@gmail.com

Abstract

The series resistance of signal and return paths in circuit board transmission line traces changes with frequency due to what is commonly referred to as the skin effect. This behavior dominates the conductor losses in interconnects above 5 Gbps. In this paper we introduce a new technique to measure the frequency dependent resistance and loop inductance of circuit board traces and compare the measurements to predictions from a popular 3D full wave solver.

Authors Biography

Eric Bogatin is currently the Dean of the Teledyne LeCroy Signal Integrity Academy, at www.beTheSignal.com. Additionally, he is an Adjunct Professor at the University of Colorado - Boulder in the ECEE dept and the editor of the Signal Integrity Journal. Bogatin received his BS in physics from MIT and MS and PhD in physics from the University of Arizona in Tucson. He has held senior engineering and management positions at Bell Labs, Raychem, Sun Microsystems, Ansoft and Interconnect Devices. He has written six technical books in the field and presented classes and lectures on signal integrity worldwide.

Yuriy Shlepnev is the president and founder of Simberian Inc., where he develops electromagnetic software for electronic design automation. He received M.S. degree in radio engineering from Novosibirsk State Technical University in 1983, and the Ph.D. degree in computational electromagnetics from Siberian State University of Telecommunications and Informatics in 1990. He was principal developer of a planar 3D electromagnetic simulator for Eagleware Corporation. From 2000 to 2006 he was a principal engineer at Mentor Graphics Corporation, where he was leading the development of electromagnetic software for simulation of high-speed digital circuits. His scientific interests include development of broadband electromagnetic methods for signal and power integrity problems. The results of his research published in multiple papers and conference proceedings.

Chun-Ting "Tim" Wang Lee is currently a Ph.D candidate focusing on signal integrity research in the Electric Engineering Department at the University of Colorado, Boulder. Wang Lee received his BSEE degrees from University of Illinois at Urbana Champaign, and MSEE from University of Colorado at Boulder. In the past years, he has involved himself with studies on signal integrity and projects sponsored by industry-leading companies such as Keysight Technologies and Teledyne LeCroy. Tim is currently working on projects pertinent to PCB material property extraction.

Introduction

In high speed channels, especially when low loss laminate materials are used, conductor loss dominates over dielectric loss. As a result, accurate predictions of channel performance depend on accurate modeling of conductor loss. At DC, the current distribution in a conductor is uniform. However, above about 10 MHz in typical circuit board traces, the current density near the surface increases with the frequency, and decreases at the conductor interior.

Physically, the electromagnetic field and conductivity current are pushed out of the conductor interior to achieve minimum impedance at a given frequency. This redistribution of current causes the resistance per length to increase and the loop inductance per length to decrease. As frequency increases beyond 1 GHz, the resistance continues to increase with frequency while the loop inductance reaches a limiting value. Known as the skin effect, the continuing increase of resistance per length with increase of frequency causes the frequency dependent loss and collapses the eye due to increasing ISI jitter.

While every full wave tool can simulate these effects and offer predictions of loss based on the skin effect, we rarely see detailed analysis and direct measurements of this effect, other than as the resistance affects the attenuation. However, this is usually at frequencies well above the transition from bulk to skin effect current distribution. This is partly due to the difficulty of measuring the very small resistance per length in the presence of contact resistance and transmission line resonance behavior.

In this paper, we introduce an unconventional 2-port measurement technique for circuit board transmission lines and directly measure the frequency dependent resistance per length and loop inductance per length. In particular, we look in the frequency range from 100 kHz to 100 MHz, where the current distribution transitions from DC to skin depth limited. To show consistency between the measurements and numerical electromagnetic solutions, these same test structures are also modeled in the popular 3D full wave simulator, Simbeor. The full wave simulator will also help us observe the details of the field and current redistribution inside the conductors.

However, since the only way to achieve a good correlation between simulation and measurement is knowing the material properties and geometry features, we will introduce techniques, where practical, to extract the important features of specific interconnects from electrical measurements.

Using a custom built, precision micro Ohmmeter, we measure the sheet resistance and etch back of traces at DC and compare these measurements to those of a VNA. From the loop inductance measurements, we extract the effective dielectric thickness. And from the resistance behavior we extract the effective thickness of the traces. It is important to note that since the resistance per length and inductance per length are not sensitive to dielectric properties of the laminate, knowing the as-fabricated dielectric properties is not as important as getting the right geometric dimensions.

Using these values, we correlate the frequency dependent resistance and loop inductance between the measured and simulated values. These described techniques can be extended for use in coupons to extract geometry and material properties on any production board.

Understanding Skin Effect

The current re-distributes in the signal and return paths of a transmission line in order to minimize the impedance of the signal-return loop. At higher frequencies, the inductive impedance dominates and current re-distributes to reduce the internal self-inductance of the path. This effect of current re-distribution is called the "skin effect," because the current is concentrated in the outer surface of the conductors [1].

Using the 3D EM simulator, Simbeor, the redistribution of signal and return current can be easily seen in the color map of current density at difference frequencies.
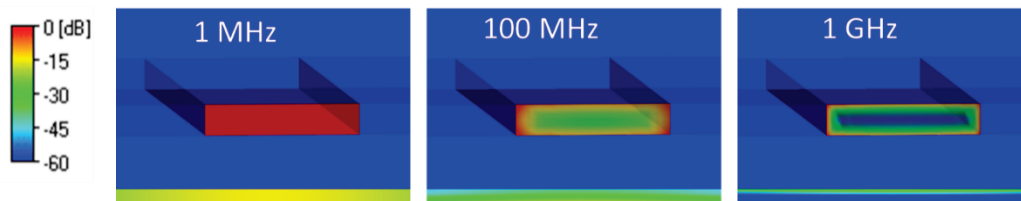

Fig. 1: Current density in a circuit board trace and its return path at different frequencies. The current in the trace starts concentrating on the curface of the trace at 100 MHz. At 1 GHz, skin effect is prominent and signal current only flows on the surface of the signal trace, and return current becomes a thin sheet of current underneath the trace.

As shown in Fig. 1, the current distribution for a stripline geometry, varies at different frequencies. At 1 MHz, at frequency low enough where skin effect is not present, the current is uniformly distributed in both the signal line and the return planes.

As frequency increases to 100 MHz, we start to see the redistribution of current in the signal line towards the surface of the conductor. At 1 GHz, we can clearly see the developed skin effect where current stays mostly on the top and bottom surface of the signal line and mostly on the side of the return planes closer to the signal.
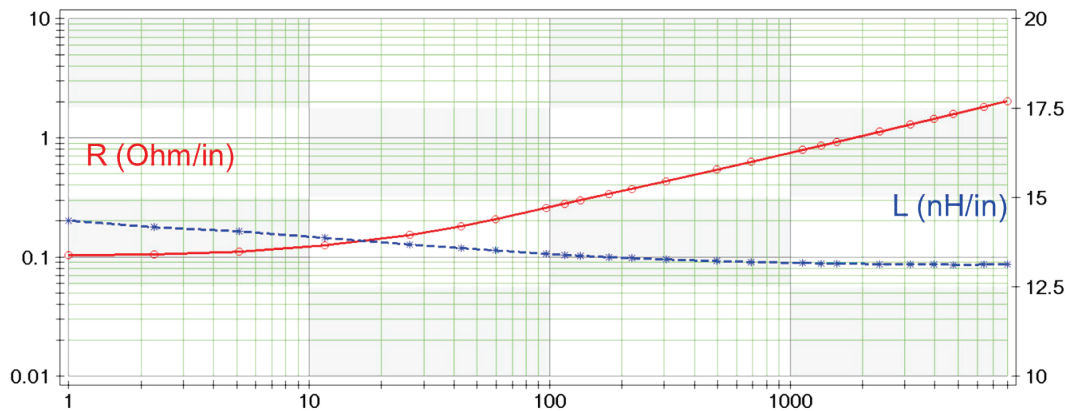

Fig. 2: Frequency depedence of resistance per inch and inductance per length. Skin effect reduces the inductance per length as frequency increases while increase the resistance per length.

The result of the current redistribution to achieve lowest inductance pushes the current to the surface of the conductor and consequently decreases the cross-sectional area, increasing the resistance. The decrease in inductance and increase in resistance is shown in Fig. 2. The impact of skin effect can be observed from how the resistance and inductance per length change with frequency.

The Sensitivity of $R_{Len}(f)$ and $L_{Len}(f)$ to Different PCB Parameters in Stripline Environment

Before delving into the process of making measurements and creating models for simulation, it is important to establish how different printed circuit board parameters impact the measurement of interest, so one knows what to expect in the measurement and simulation. To explore how different dimensions of a given stack-up and trace influences, we carry out a sensitivity analysis on a signal trace and relevant parameters in a stripline environment shown in Fig. 3.

H1: Height of substrate above trace
H2: Height of substrate below trace
W: Trace width
T: Thickness of trace
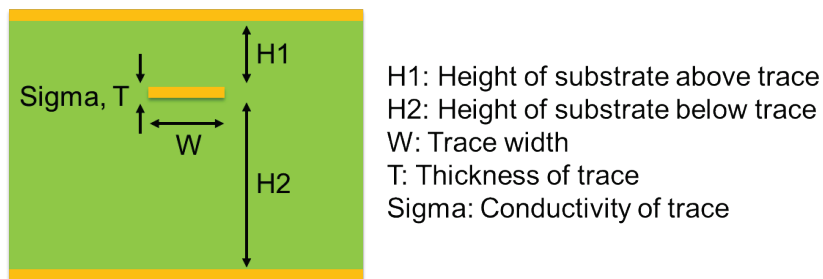Sigma: Conductivity of trace

Fig. 3: A circuit board cross-section to show different parameters to vary in the sensitivity analysis.

There are five parameters that influence the resistance per length, $R_{Len}(f)$, and inductance per length, $L_{Len}(f)$. To first order, the dielectric properties are not important because the laminates used in PCB fabrications are not magnetic and have relative permeability of unity, so inductance per length is only affected by geometry. Knowing the parameters to vary, we are now ready to conduct the analysis. The analysis consists of applying the same percentage of change to each of the parameters listed and observing the deviation of the two curves from the nominal value.
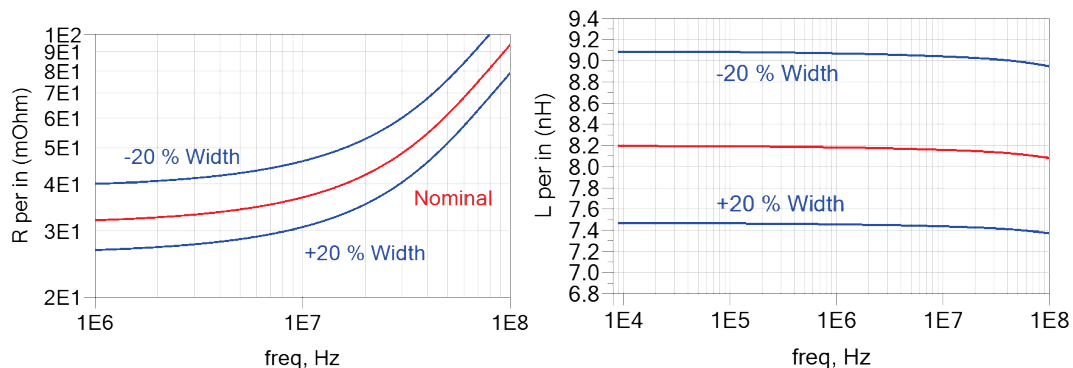
1. Sensitivity to Width Variation

Fig. 4: Resistance per length and inductance per length curve with 20% width change. Both resistance and inductance curve are sensitive to the width of the trace.

First, we take a look at how width variation changes the behavior of resistance per length and inductance per length. It is expected that compared to the nominal value, a wider trace width has lower resistance and lower inductance while narrower trace width produces higher resistance and inductance.

The resistance per length and inductance per length curves in Fig. 4 show consistent results with expectation. Moreover, it indicates the importance of the correct trace width, for both resistance and inductance are sensitive to width variation; a ±20% change in width translates to ±20% change in resistance and about ±10% change in inductance.

2. Sensitivity to Substrate Heights

Second, we vary the substrate height above and below the signal trace and observe the changes in the resistance and inductance curves. On one hand, we expect changing the substrate heights to have little to no effect on the resistance curve since most of the current resides in the conductor of the signal line.

On the other hand, the height of the substrates should affect inductance curve because the amount of mutual inductance is determined by the distance between the signal and return path: the closer the signal to the return path the higher the mutual inductance, lower the total inductance [2] [3]. In addition, there should be more impact when H1, the distance to the closer return path, is changed.
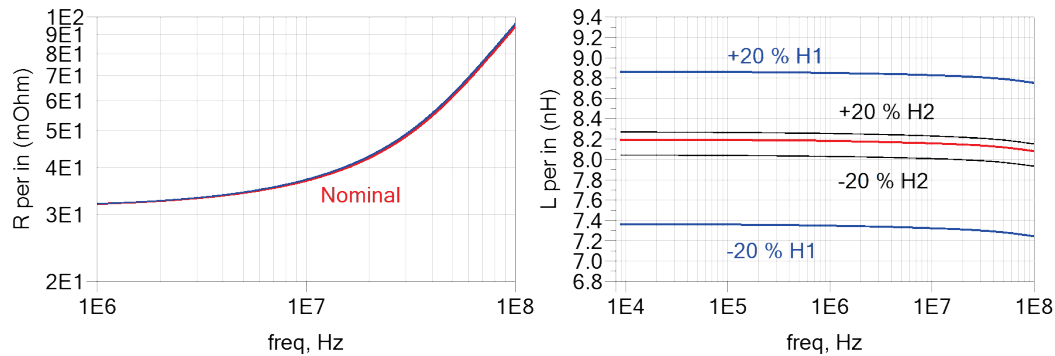

Fig. 5: Resistance per length and inductance per length curve with 20% substrate height change. The inductance curve is siginificantly more sensitive to the change of subtrate heights.

Shown in Fig. 5 are results of varying H1, height above trace, and H2, height below trace. As expected, the 20% variation of both substrate heights has little to no effect on the resistance curve, and the variation in inductance by changing H1 is significantly more than changing H2.

Specifically, a 20% change of H2 only affects the inductance per length by at most 2.5%, but a 20% change in H1 changes the inductance by more than 10%. Since the inductance curve is more sensitive to H1, H2 is considered fixed and will not be adjusted.

3. Sensitivity to Conductivity and Thickness

Finally, we show how sensitive the resistance and inductance curves are to the conductivity and thickness of the signal line. At DC, the resistance per length is

$$R_{Len} = \frac{1}{\sigma} \frac{1}{W \cdot t}$$ (1)

From the DC unit length resistance shown in (1), we can expect, at low frequency, the same percentage change of the conductivity and thickness influence the resistance curve the same way. Nonetheless, as frequency increases to the onset of skin effect and current starts to redistribute itself, the frequency dependent resistance per length becomes

$$R_{Len}(f) = \frac{1}{W} \sqrt{\frac{\mu_0 \pi f}{\sigma}},$$ (2)

Once the frequency is high enough and skin effect is prominent, the change in thickness and conductivity would present themselves differently in the resistance curve. Moreover, since inductance is independent of conductivity, the inductance curve should stay the same even with different conductivity, and thicker conductor has lower inductance.
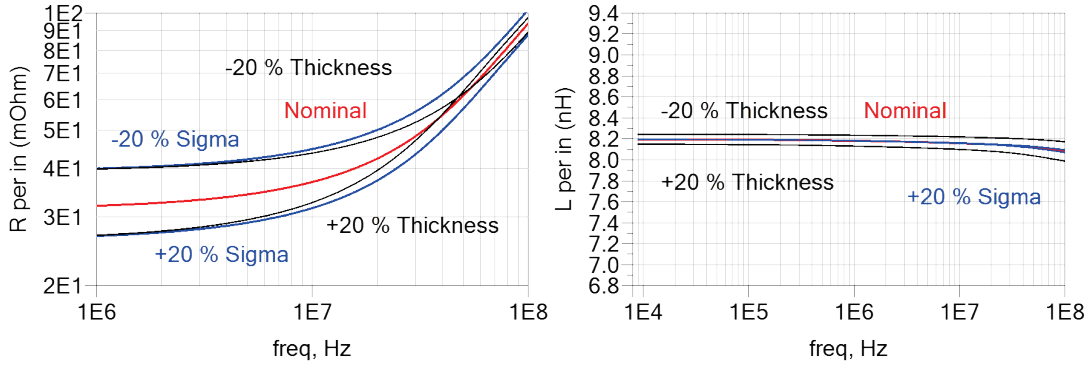

Fig. 6: Resistance per length and inductance per length curve with 20% thickness and conductivity change. Resistance curve has different frequency dependency with respect to thickness and conductivity change, while small inductance change is seen by changing the thickness.

The resistance curve on the left of Fig. 6 shows the expected different frequency dependence from conductivity and thickness variation. The inductance curve on the right of Fig. 6 informs us inductance is not sensitive to conductivity, but it is sensitive to thickness (although only 1% inductance change from 20% thickness change).

Reducing Number of Variables

Having seen how five different parameters influence the resistance and inductance curve differently in the sensitivity analysis, we shall see if we can reduce the number of variables. To do so, we revisit the expression for resistance,

$$R = \frac{1}{\sigma} \frac{len}{Area}.$$ (3)

Rewriting (3) with the assumption of a rectangular conductor, we have

$$R = \frac{1}{\sigma} \frac{len}{W \cdot t},$$ (4)

where W is the width of the conductor, and t is the thickness. Reorganize terms and introduce the sheet resistance, $R_\square$, (4) becomes

$$R = \frac{1}{\sigma \cdot t}\frac{len}{W} = R_\square \cdot \frac{len}{W},$$

$$R_\square = \frac{1}{\sigma \cdot t}.$$

(5)

After the manipulation, we have combined conductivity and thickness into a new term: the sheet resistance. Since the sheet resistance is the inverse of the product of conductivity and thickness, once we measure the sheet resistance, it only requires one of the two variables to compute the other.
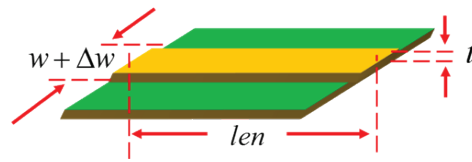
Fig. 7: Illustration of a circuit board trace with small width change from nominal value.

Furthermore, to include the change in nominal trace width during fabrication as shown in Fig. 7, we add a correction term ΔW to the width in (5) and take the inverse:

$$R = R_\square \frac{len}{W + \Delta W}$$

$$\frac{1}{R} = G = \frac{1}{R_\square \cdot len}(W + \Delta W)$$

(6)

The last equation in (6) states that the conductance is a linear function of trace width, and the slope is a function of sheet resistance.
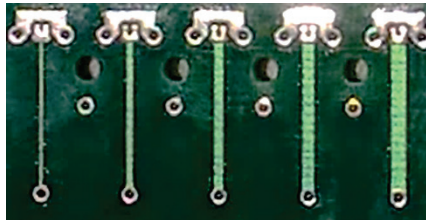

Fig. 8: A set of microstrip test lines with five different widths to perform sheet resistance and width variation extraction.

Using the insight learned by examining the equation for conductance, we designed a set of strip line test patterns with five different trace widths and of the same length (a microstrip example is provided in Fig. 8). The sheet resistance, $R_\square$, and the width correction term, ΔW would be extracted by fitting a linear function through the conductance data points. Using the 5 lines, the values $R_\square$ and ΔW can be extracted, and the original five variables are now reduced to three: thickness and the substrate heights.

Potential Artifacts: Constricting Current and Via

To enable the use of an industry standard SET2DIL probe in the later measurements, the SET2DIL footprint was incorporated in the test pattern. The same SET2DIL pattern is serving as the feed-in for lines of five different trace widths. There can be a potential artifact of current constricting at the feed-in and in the via shorts at the end. Moreover, since the test lines are in the strip line layer, via transitions are necessary to probe the lines from the surface.
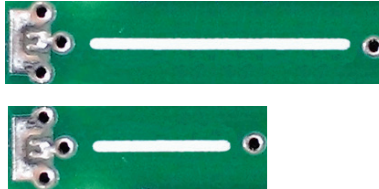
Fig. 9: A long line and a short line of the same trace width. By taking the difference of the two, we eliminate potential via resistance and constricting current artifact.

To eliminate the potential artifact in the vias and feed-in, two different lengths of the same width test lines were fabricated, see Fig. 9. By taking the difference of the longer line and the shorter line, we would be able to remove these artifacts and their frequency dependent behavior.

Test Pattern Dimensions

An example of the stripline test pattern shown in Fig. 9. The longer line is 1.3 inches while the shorter line is 0.3 inches, measured from the center of the first via to the shorting via at the end. Each of the long and short lines have five different widths ranging from 6 mils to 30 mils with 6-mil step.

Given the dimensions and general sheet resistance value for 1 oz copper, 0.5 mOhm per square, we can approximate the lowest resistance value expected using the shortest and widest line. With width 30 mils and length 0.3 inches, there are 10 squares for the shortest and widest line, which translates to 5 mOhm.
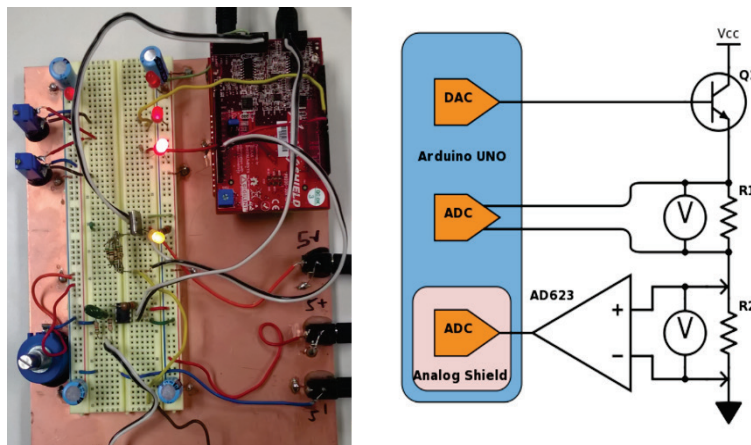

Fig. 10: A picture of the custom built precision micro-Ohm meter and its system block diagram.

Precision DC Measurement with a Low Cost Custom Micro-Ohm Meter

To eliminate the impact of contact resistance and effectively measure DC resistance down to the milli-Ohm range. We built a precision microOhm-meter with its system diagram shown in Fig. 10.

In summary, a microcontroller is used to send voltage to the bipolar junction transistor to source a test current. The value of the test current is then measured by taking the ratio of the measured voltage across a well characterized sense resistor. As the same test current goes through the device under test, a differential amplifier is in place to increase the signal to noise ratio of the measured voltage across the DUT. Lastly, the resistance under test is calculated by taking ratio of the measured device voltage and the measured test current.
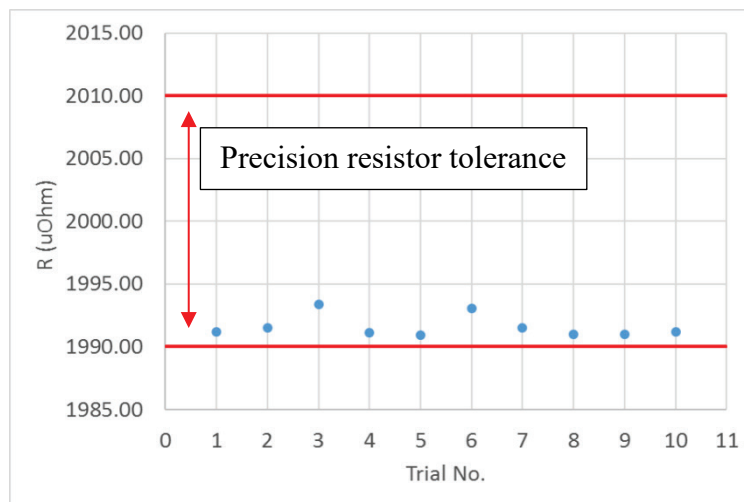

Fig. 11: A measurement of a precision 2 mOhm, 0.5% resistance with the custom built micro-Ohm meter. The precision micro-Ohm meter accurately measures a 2 mOhm, 0.5% precision resistor with difference between each measurement down to less than 0.25%.

In addition to the four-point kelvin connection to eliminate contact resistance, numerous design features are also in place to compensate for thermal EMF, reduce self-heating of sense resistor and increase the precision of the measurement. Shown in Fig. 11 is ten consecutive measurements of a 2 mOhm, 0.5% precision resistor by the micro-Ohm meter. The custom built micro-Ohm meter has accurately measured the 2 mOhm resistance with a difference less than 0.25%. between each measurement.
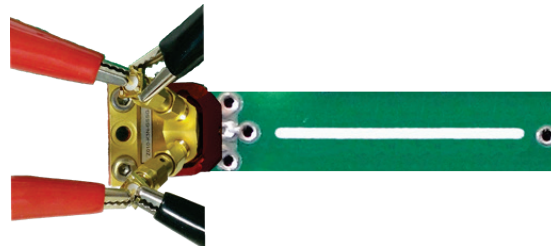
DC Measurement Results

Fig. 12: DC measurement of a test line with SET2DIL probe as fixture.

With the described micro-Ohm meter, we measured the resistance of the long lines and the short lines using the SET2DIL microprobe as a fixture, as shown in Fig. 12. The resistance of the 1-inch section without via or feed is then calculated by taking the difference between the measured long and short lines.
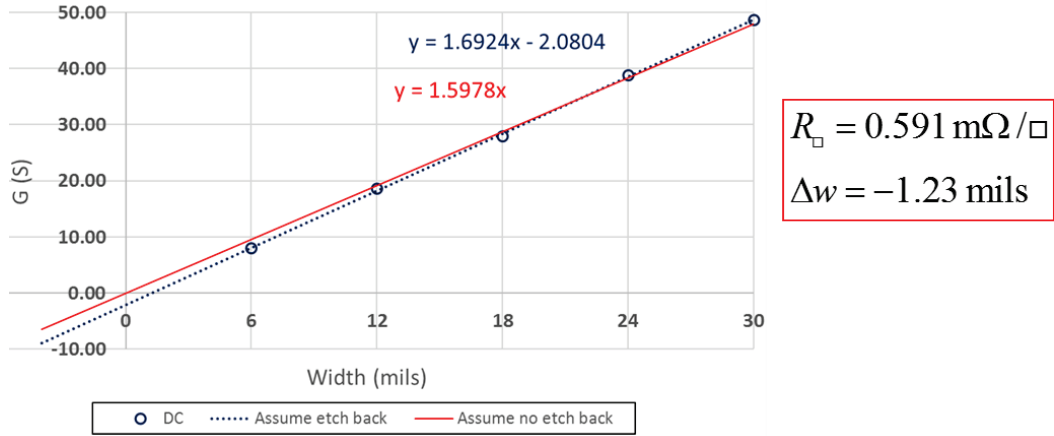

$$R_\square = 0.591\,\mathrm{m\Omega}/\square$$

$$\Delta w = -1.23\,\mathrm{mils}$$

Fig. 13: Extaction process of sheet resistance and width variation. The extracted sheet resistance is 0.591 mOhm per square and the width variation is negative 1.23 mils. The red trend line demonstrates the need for the correction term to have a good model to fit the conductance data points.

Following (6), to back out sheet resistance and width change, we calculated the conductance of each width and fitted a linear function through the conductance data points, shown in Fig. 13. The value extracted for sheet resistance is 0.591 mOhm per square: consistent with the rule of thumb for 1 oz copper, 0.5 mOhm per square.

Etch Back is a Significant Term

To make sure a delta width change is necessary for the given conductance data points, we also fitted another trend line without an assumed width change. The fit of the two models are then compared by calculating the difference between values predicted by the model and measured values.
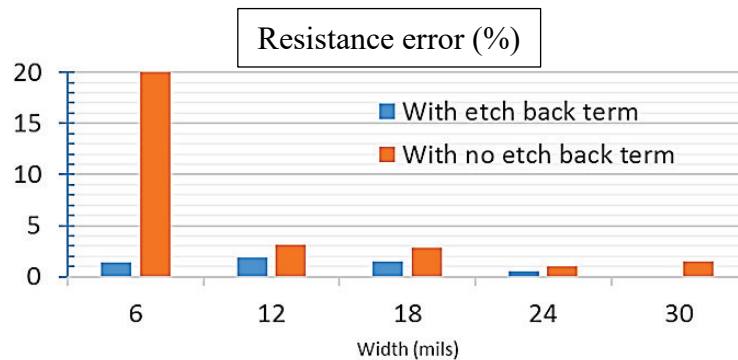

Fig. 14: Resistance error of two different models. With an etch back term in the model, the resistance error is less than 3%. Without an etch back term, there is a 20% resistance error for the narrowest line.

Seen in Fig. 14, while the values predicted by the model with etch back term has less than three percent difference compared to the measured values, the resistance difference

between the values predicted without the etch back term is as large as 20%. The result of the comparison between the two models confirms the need for the etch back term.

The value of -1.23 mils means the actual line width is consistent with a line width that is thinner than the as designed line width by 1.23 mils. This is about the amount of etch back expected in an isotropic subtractive process. The etch back will be comparable to the thickness of the trace.

How consistent is the extracted values?

It should be noted that the series resistance extracted for the 1-inch length of trace from the RF test pattern includes the series resistance of the return path. This RF test pattern with a shorting via at the end, measured at DC, cannot separate the contribution from the signal path and return paths.
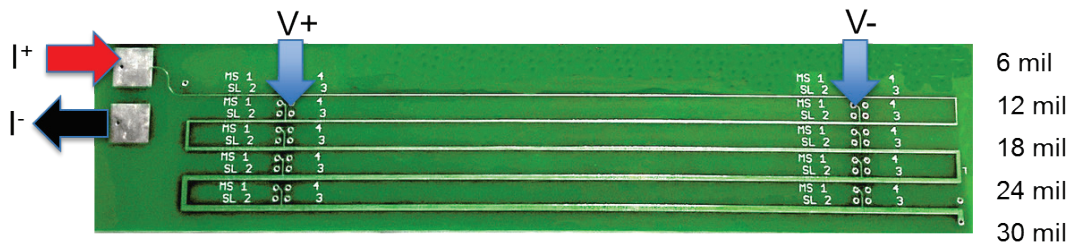

Fig. 15: DC test lines for sheet resistance and width variation consistency test.

Another pattern was designed and measured that included just the signal trace on the same layer on the same board. This different test structure is shown in Fig. 15. It is a series of 3-inch lines of different widths on different PCB layers.

The same current is forced through all the lines and the voltage drop across the 3-inch uniform trace is measured. The widths' progression is identical to the previous test structures: starting from 6 mils to 30 mils with 6-mil step. The same algorithm was applied to the resistance measured to extract sheet resistance and etch back.

Board No.	$R_\square$ (mΩ/□)	Δw (mils)
1	0.579	-1.00
2	0.577	-0.94
3	0.581	-1.14
4	0.581	-1.10

Across boards

	Average	SET2DIL	Variation
$R_\square$ (mΩ/□)	0.579 ± 0.5 %	0.591	2.0%
Δw (mils)	-1.05 ±10 %	-1.23	17%

Fig. 16: Tabulated results of extracted sheet resistance and etch back from the DC test pattern from four different boards. The measured sheet resistance from the RF pattern is 2% higher than the value from the average of the sheet resistance extracted from DC test lines.

We examined a total of four different boards and the extracted values for sheet resistance and etch back are tabulated in Fig. 16. The etch-back extracted from the RF test lines is 17% more than the average etch back value of four different boards. This is an indication of the variation from different regions on the same panel.

The extracted sheet resistance in the DC test patterns varied by less than 0.5% across the samples. This is consistent with the measurement of the distribution of sheet resistances

in a panel of copper foil. An 18-in x 24-in panel was partitioned into 54 2-inch by 2-inch squares and the sheet resistance in each square measured with a 4-point probe.
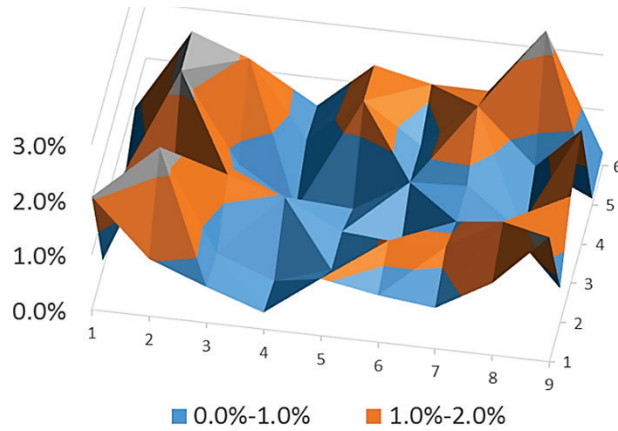

Fig. 17: A spatial map of a measured sheet resistance difference in percentage of a panel of standard copper foil. In the middle of the panel, where there is no current crowding effect, the difference in sheet resistance is less than 1%.

Shown in Fig. 17 is a spatial map of the sheet resistance in percentage in comparison to the average sheet resistance calculated excluding the values from edges and corner. The higher resistance in the corners and by the edge is a measurement artifact due to the edges of the board crowding the current. The sheet resistance across a panel varied by less than 1%.

However, the sheet resistance measured in the RF test structures was still higher than measured in the DC test structures by about 2%. We believe this variation is due to the contribution from the return path in the RF test patterns which was not present in the DC test patterns.

To verify this, two experiments were conducted in Simbeor, a Full wave 3D EM solver. A stripline of a fixed length was simulated and sheet resistance extracted in two cases; the only difference between the two cases was the conductivity of the return planes.
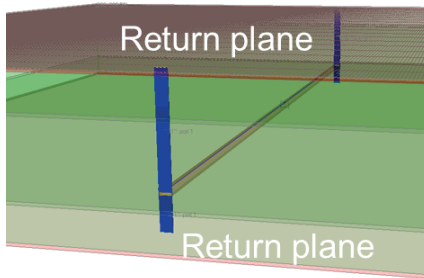
	Return plane		
	PEC	Copper	Differece
R sheet (mOhm/sq)	0.588	0.601	2.20%

Fig. 18: Simulation setup and result of a stripline trace with different return planes. The sheet resistance between a signal line with copper return plane is 2% higher than a signal line with ideal return plane.

Shown in Fig. 18, the result of the experiment confirms that the 2% difference in the RF structure measurement is indeed caused by the return plane. The consistency between the simulation and measurement confirms our speculation that the sheet resistance between

the DC lines and RF lines are different because of the return planes associated with the RF lines.

Residual from Via and Feed-in Artifact

To examine the impact from the via resistance and feed-in on the resistance, we subtracted the resistance of the nominal via-to-via length of transmission line under test using the extracted sheet resistance and the line width.

Given the via diameter of 15 mils, with a 45 mil circumference and the substrate height, 40 mils, we expected the via resistance to be in the range of 1-2 mOhm, and about the same amount of resistance contribution from the constricting current at the feed-in.

width (mil)	R residual mOhm	
	0.3 in	1.3 in
6	2.24	4.00
12	8.64	7.57
18	10.12	10.64
24	10.46	10.32
30	10.19	10.20

Fig. 19: Residual resistance calculated by subtracting the resistance of a 0.3-inch line and a 1.3-inch line. The residual resistance of different trace widths of different lengths are comparable to each other.

However, shown in Fig. 19, the result of the residual resistance after subtracting the section of line shows a much higher residual resistance. This pattern suggests a significant redistribution of current when the geometry changes. The details will be investigated in a follow-on study.

Road to $R_{Len}(f)$ and $L_{Len}(f)$

Having extracted and confirmed the consistency of the values of sheet resistance and the width change, we have successfully reduced the five different variables- width, height above substrate, height below substrate, conductivity and thickness-to three: the heights of the substrates and the thickness of the trace. The remaining three variables are extracted by fitting a model to the measured resistance per length and inductance per length curve of the RF test structure.

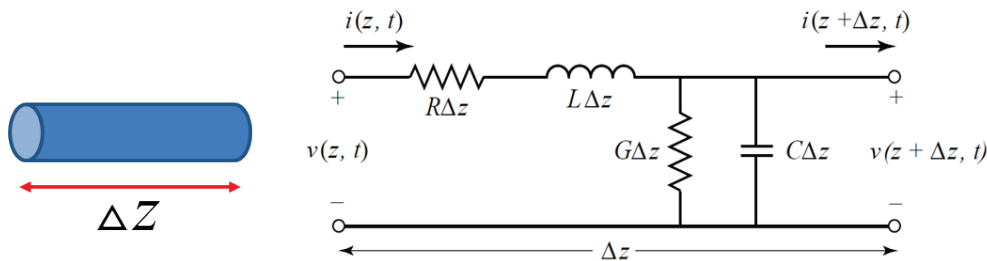### RF Structure for $R_{Len}(f)$ and $L_{Len}(f)$ Extraction

Fig. 20: An illustration of the lumped element model of a transmission line of infinitesimal length.

The resistance and inductance per length curve can be extracted by taking advantage of the lumped element model of a transmission line. A transmission line is often schematically represented as a two-wire line since transmission lines (for transverse electromagnetic [TEM] wave propagation) always have at least two conductors [4]. The piece of line of infinitesimal length $\triangle z$ is modeled as a lumped-element circuit, as shown in Fig. 20, where R, L, G, and C are per-unit-length quantities.

To investigate the resistance per length and inductance per length, the RF test structure is shorted at the end. By shorting the end of the transmission line, the input impedance at frequencies well below the transmission line ¼ wave resonance is effectively the frequency dependent resistance and inductance per length curves.

Expected R$_{Len}$(f) and L$_{Len}$(f) from Shorted Tline
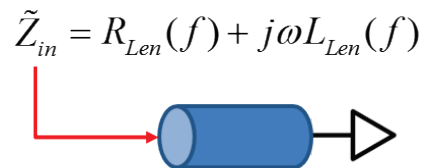
$$\tilde{Z}_{in} = R_{Len}(f) + j\omega L_{Len}(f)$$

Fig. 21.Simple model of the input impedance of the transmission line in terms of the lumped resistance and inductance.

As shown in Fig. 21, the input impedance of a shorted transmission line is equivalent to a frequency-dependent resistance and frequency-dependent inductance connected in series. If they are in the lumped circuit regime, the per unit length terms can be used, given the length. Once the input impedance is identified, the real part of the input impedance of the series network is the resistance per length and the imaginary part is related to the inductance per length.
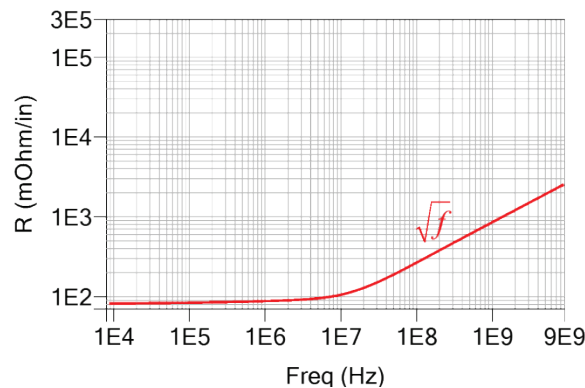
Fig. 22: The ideal frequency dependency of resistance per length of a shorted transmission line of infinitesimal length.

Ideally, the resistance per length curve should stay relatively constant at low frequency and as frequency increases, scales with the **square root** of frequency when the skin effect becomes prominent as shown in Fig. 22. On the other hand, the inductance per length curve is the quotient of the imaginary part of the input impedance and the angular frequency. The inductance should decrease as skin effect takes hold and more current

concentrates on the surface of the conductor. When all the inductance is external, the inductance per length reaches a constant value.

Although it might seem straightforward to convert an input impedance reading to resistance per length and inductance per length using the method prescribed, there are many practical challenges in acquiring the input impedance measurement.

Achieve Low Level Measurement with the 2-port Technique

Given the geometry of our test structure, the estimated resistance is about 15 mOhm. In a 1-port measurement, the S_{11} value for such a resistance structure is then

$$S_{11} = \frac{R_{DC} - 50}{R_{DC} + 50} \approx -0.005 \, dB. \tag{7}$$

This regime of low resistance/impedance is difficult to measure in practice with a conventional 1-port VNA due to real world limitations of signal to noise ratio and fixture reproducibility [5].
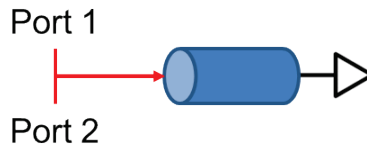

Fig. 23: Port configuration of the 2-port low impedance measurement.

Consequently, an alternative RF technique for measuring low resistance is used. This unconventional 2-port ultra-low impedance measurement technique is analogous to the four-point kelvin technique. In this case, both ports are connected to the same node. Port 1 excites the device under test while port 2 measures the response from the excitation, shown in Fig. 23.

With a 50 Ohm reference port impedance, the input impedance of the 2-port measurement is calculated as

$$Z_{in} = 25 \frac{S_{21}}{1 - S_{21}}. \tag{8}$$

Using the estimated resistance 15 mOhm as the input impedance in (8) and solving for S_{21}, we arrive at -64 dB, a value that is more measureable than -0.005 dB.

Tline Resonance Artifact:

Given a length of a shorted transmission line, the input impedance can be expressed as

$$Z_{in} = jZ_0 \tan(\gamma \cdot len), \tag{9}$$

where Z_0 is the characteristic impedance of the line, γ is the complex propagation constant and *len* is the length of the transmission line. The tangent function in (9) causes a periodic resonant behavior in the input impedance whenever the length of the line is a multiple of a quarter of a wavelength.
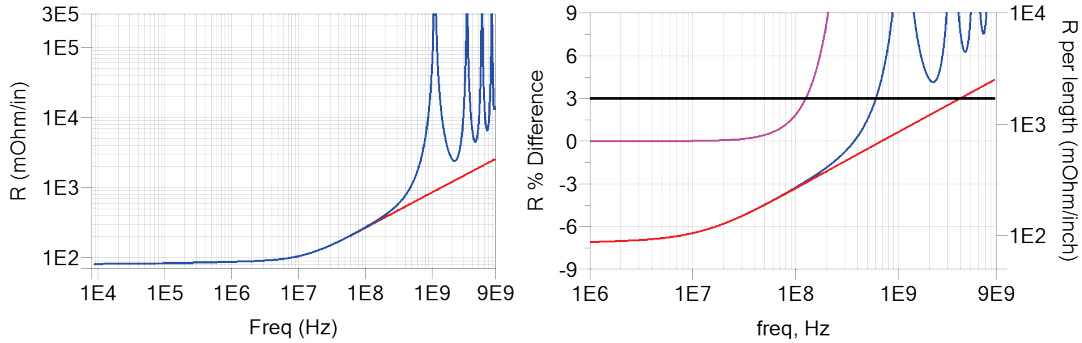

Fig. 24: Left: the resonant transmission line effect of a 1.3-inch line in blue in comprison with a line of infinitesimal length. Right: below 150 MHz, the transmission line effect introduces less than 3% resistance difference.

Because of this quarter wave length resonance, the shorted transmission line looks like an open circuit at different frequencies depending on the physical length of the line: longer the line, lower the first resonant frequency. Shown in Fig. 24, for our longer 1.3-inch line, the resonant behavior starts producing an artifact in the interpreted resistance per length greater than 3% above 150 MHz. This frequency determines the bandwidth of our data with less than 3% of the transmission line effect artifact.
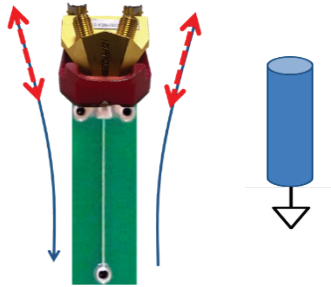
Probe Length Artifact:

Fig. 25: Illustration of additional phase introduced by SET2DIL probe in the measurment.

In addition to the transmission line effect, the extended length microprobe, shown in Fig. 25, also contributes a significant artifact in the extracted resistance. The presence of the probe length adds extra phase to the measurement of the device under test. To examine the impact of the phase, we first express the input impedance in terms of magnitude and phase, $\tilde{Z}_{in} = \left| \tilde{Z}_{in} \right| e^{j\varphi}$, and then find the resistance by taking the real part of the input impedance:

$$R = \left| Z_{in} \right| \cos(\varphi). \tag{10}$$

From (10), it is clear that the extracted resistance is indeed a function of phase.
To see the effect in measurement, we took the real part of the input impedance to observe
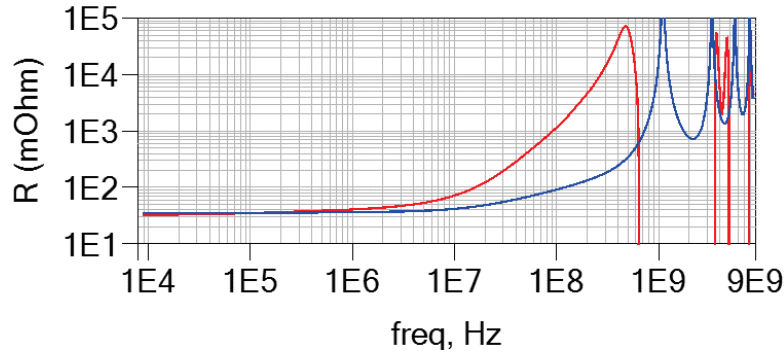

Fig. 26: Resistance per length curve that shows an order magnitude increase of resistance introduced by the phase shift from the extended length probe.

the impact of the probe length on the extracted resistance after taking the measurement of the 1.3-inch line and using (8) to convert S_{21} to input impedance.

The red curve shown in Fig. 26 is the extracted resistance per inch in comparison with the ideal 1.3-inch line including transmission line effect. The presence of the probe length increases the resistance by as much as an order of magnitude in the frequency regime of interest. To eliminate this resistance artifact associated with the probe length, proper de-embedding should be done to the measurement before calculation of the resistance and inductance curves.
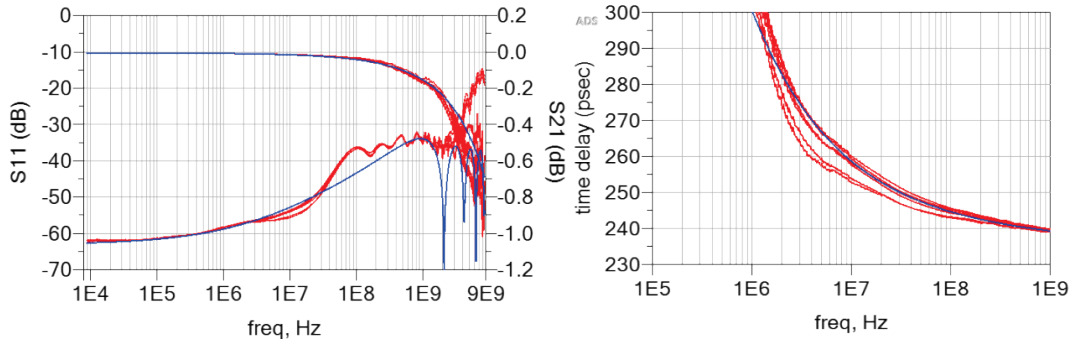
De-embedding with 2x thru reference structures

Fig. 27: Measurement of six nominally identical thrus. Although the S_{11} and S_{21} are quite similar, there is as much as 10 psec time delay difference in the MHz range.

To de-embed the probe, six nominally identical 2x thrus were measured and modeled. However, seen in Fig. 27, the nominally identical fixtures are quite different in terms of time delay, which is the important term that determines the anomalous phase shift from the fixture. There is as much as 10 psec difference between the thrus.

To see how the difference in probe length affects the resistance per length curve, we express R in terms of the time delay and arrive at

$$\frac{\Delta R}{R} = \frac{\omega L}{R}\Delta TD \cdot 2\pi f. \tag{11}$$

Using an inductance estimate (10 nH/in), estimated resistance of 15 mOhm and given dimensions of the test patterns, we plot (11) in Fig. 28. As shown, at 100 MHz, with 1 psec <u>total</u> delay, there is more than a 5% difference in the relative resistance.
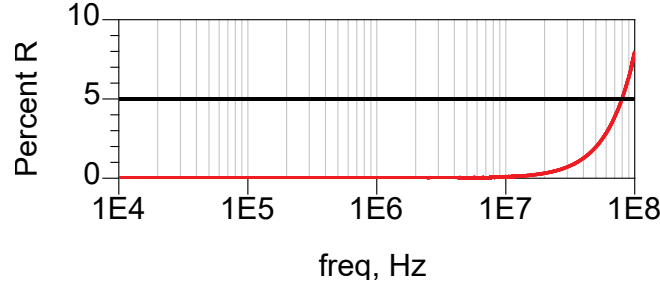

Fig. 28: Resistance difference plot in percent. At 100MHz, there is more than 5% resistance difference introduced by the 1 psec total delay.

Having shown the calculation of the impact of the time delay, the 10 psec difference in nominally identical fixtures might seem to be a showstopper. However, with the novel negative length de-embedding technique introduced in a later section, one is able to adjust the de-embedding element to different lengths to accommodate these fixture differences.

Non-physical Phase Behavior After De-embedding

Although the negative length de-embedding technique allows the user to adjust the length of the de-embedding transmission line to lower possible resistance difference, it is important to guarantee the de-embedded measurement remains physical.

To ensure physical behavior, we rewrite (8) in terms of measured S-parameter and examine the phase of the impedance:

$$\varphi = \angle \tilde{Z}_{in} = \tan^{-1}\left(\frac{\sin(\theta_{21})}{\cos(\theta_{21}) - \left|\tilde{S}_{21}\right|}\right). \tag{12}$$

According to (12), for the de-embedded result to be physical after de-embedding, the phase of the input impedance has to remain between ±90 degrees, for that is the range of inverse tangent function.
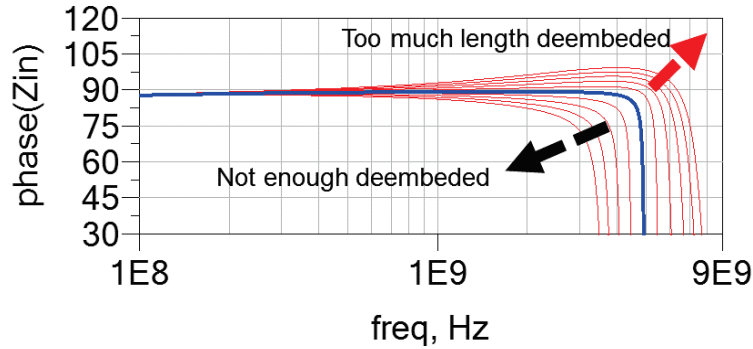
Fig. 29: Observed non-physical behavior when de-embedding length is too much.

Fig. 29 shows how the ideal phase (in blue) in comparison with too much de-embedding and not enough. A good de-embedding process, then, is one that de-embeds enough probe length, so the maximum phase of the input impedance is less than 90 degrees.

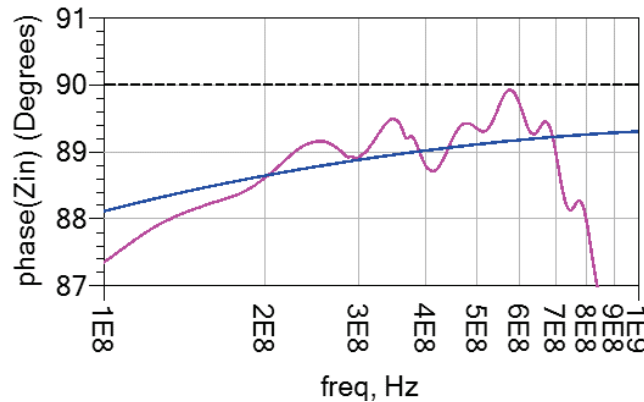## Artifact: Noise in the Phase After De-embedding

Fig. 30: De-embedded result with numerical noise in the phase of the input impedance.

As seen in Fig. 30, while the de-embedding process has been tuned so that the phase of the input impedance is under 90 degrees, there are ripples in the phase because of the numerical nature of the de-embedding process.
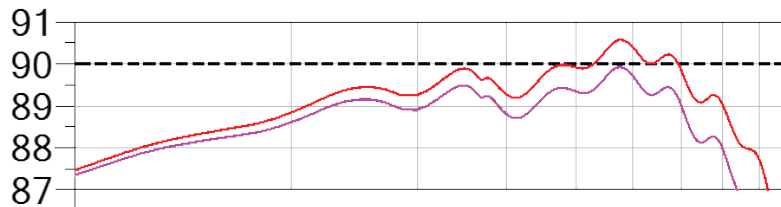

Fig. 31: Example of de-embedding input impedance phase to the peak and valley to examine the resistance change.

To see the consequence of the numerical noise in phase after de-embedding, we examined the difference in resistance when we adjust the negative length of the transmission line to de-embedded up to the peak of the ripple and when we de-embed to the first valley of the ripple, as shown in Fig. 31.
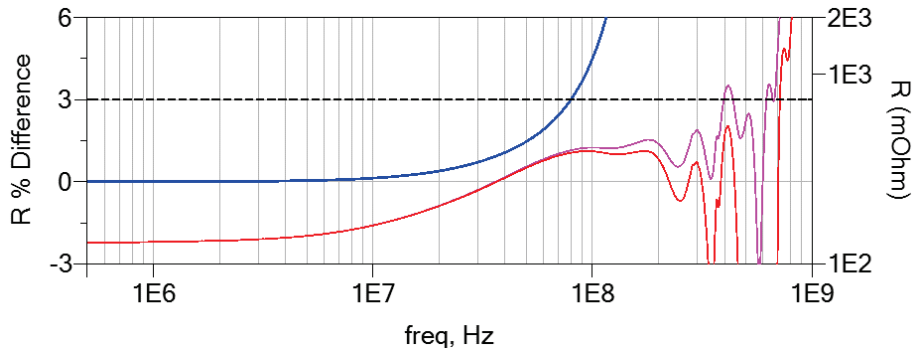
Fig. 32: Plot of resistance difference when de-embedding to the peak and the valley. To have a 3% resistance difference or below, the bandwidth of the deembedded measurement is about 80 MHz.

The resistance curves after de-embedding the two extreme cases are shown in Fig. 32, as well as the percent difference in resistance of the two de-embedding configurations. Choosing 3% as the tolerance of the resistance difference, the valid bandwidth of de-embedded measurement is 80 MHz.

Negative Length Tline De-embedding Technique

A simple transmission line model was used to fit the measured 2x thru structures. This model was then inverted by setting the length to a negative value. Surprisingly, this simple model is all that is needed to de-embed the fixture from the 2-port measurement.

The advantage of this technique is that it allows the flexibility to finely adjust the length in real time to keep the phase of the impedance out of the on-physical regime. This negative length transmission line element, as a simple de-embed element, and has been verified in other simulations.
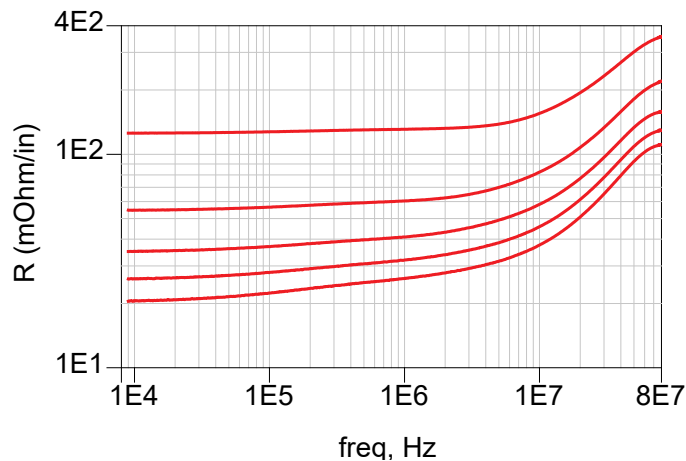
Consistency of De-embedded RF Measurements

Fig. 33: de-embeded measurments of five lines of different widths.

Shown in Fig. 33 is the result of taking the difference between the measured de-embedded 1.3-inch line and 0.3-inch line. The five different curves correspond to five different widths prescribed in the sheet resistance measurement. Since the start frequency of the RF measurement is low enough such that the current in the trace is uniformly

distributed, we made a comparison between the RF measurement at 10 kHz and the DC measurement.

	Resistance per inch (mOhm)	
w (mil)	DC	RF
6	125.6	125.5
12	53.8	54.7
18	35.8	35.0
24	25.8	26.0
30	20.6	20.5

	R sheet	delta W
DC	0.591	-1.23
RF	0.589	-1.26

R_{sheet}: 0.3%, Delta W: 2.7%

Fig. 34: Resistance per inch comparison of DC measurement and RF measurement at low frequency. The consistency between the measured results with precision micro-Ohm meter and RF measurement establish validity of our measurement and data at DC.

Fig. 34 shows the comparison between the DC measurement of the RF structure and lower frequency readings of the RF measurement. Using the same method for extracting sheet resistance and delta width change, we also calculated the values for sheet resistance and etch back from the RF measurements. The extracted sheet resistance and the delta width change are no more than 3% different than each other, confirming the consistency of our approaches.

Preliminary Simulation and Measurement Correlation

Shown in Fig. 35, by using a thickness of 1.19 mils and conductivity of $5.6 \cdot 10^7$ S/m, and nominal substrate heights and dielectric properties from vendor, we achieved a good fit for the inductance per length from 50 kHz to the upper limit of 80 MHz.
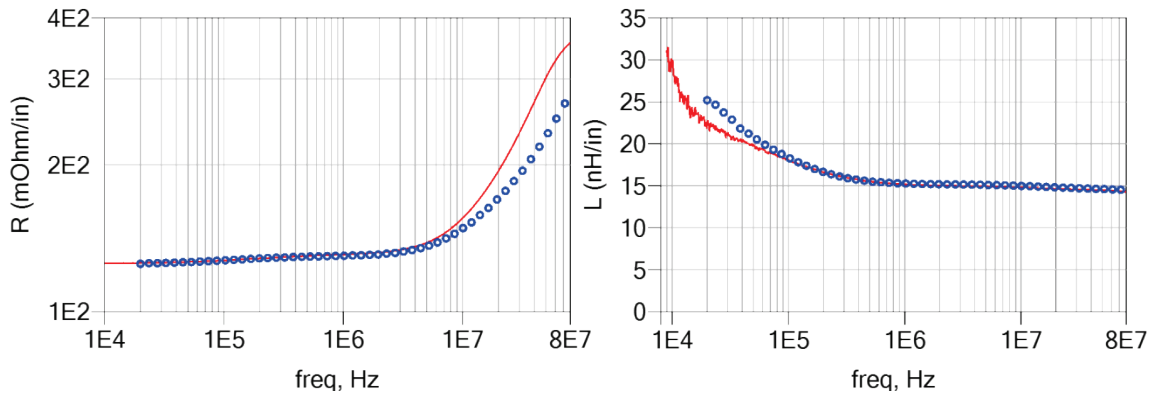

Fig. 35 Measurement (red) and simulation (blue) match of 6-mil wide line from 9 kHz to 80 MHz. The resistance curve matches quite well at low frequencies, but has a different shape after skin effect turn-on.

The measured resistance per length matches the simulated resistance per length very well from the low frequency end to about 10 MHz, where the skin depth is beginning to turn on. Currently, we are investigating the cause of this difference in shape of the resistance per length curve after turn-on of skin effect.

Summary

In this paper, we revisited the physics of skin effect and its effect on resistance per length and inductance per length. To help a better correlation between measured and simulated

skin effect, we examined how different geometry parameters in a stripline stackup affect the resistance per length and inductance per length curve.

We have shown that the 5 lines technique is an effective way to extract sheet resistance and line width variation in the as-manufactured traces. To measure the DC resistance of lines with resistance in the milli-Ohm range, we developed a novel micro-Ohm meter that is insensitive to contact resistance and thermal EMF, and is able to measure resistance with excellent accuracy and repeatability.

In comparing the sheet resistances extracted from different structures, we identified a 2% contribution from the return path conductivity to the sheet resistance.
In addition, our 5-line test pattern was designed with a SET2DIL footprint so that the manual microprobes could be used. The techniques discussed in this paper can be easily extended for use in coupons to extract geometry and material properties on any production board.

To make low level RF measurement to extract resistance down to milli-Ohm range, we have shown an unconventional 2-port technique that is also insensitive to contact resistance. To de-embed excess fixture from the measurement, a unique negative length de-embedding technique was introduced. On top of the de-embedding technique, different criterion for the 5-line de-embedding workflow was established for the conversion from S-parameter to resistance and inductance per length curve.

We will continue to analyze the measurement and simulation correlation at the turn on of the skin effect.

Acknowledgement

Reference

[1]   H. a. Wheeler, "Formulas for the Skin Effect," *Proc. IRE*, vol. 30, no. 9, pp. 299–311, 1942.
[2]   E. B. Rosa, "The self and mutual-inductances of linear conductors," *Bulletin of the Bureau of Standards*, vol. 4, no. 2. p. 301, 1908.
[3]   E. Bogatin, *Signal and Power Integrity Simplified*. 2004.
[4]   D. M. Pozar, *Microwave Engineering*, 4th ed. 1997.
[5]   Agilent Technologies, "Agilent Ultra-Low Impedance Measurements Using 2-Port Measurements Application Note," 2007.